

# Tibial stress during running following a repeated calf-raise protocol

Hannah M. Rice<sup>1</sup>  | Megan Kenny<sup>1</sup> | Matthew A. Ellison<sup>1</sup>  | Jon Fulford<sup>2</sup> |  
Stacey A. Meardon<sup>3</sup>  | Timothy R. Derrick<sup>4</sup>  | Joseph Hamill<sup>5</sup>

<sup>1</sup>Sport and Health Sciences, University of Exeter, Exeter, UK

<sup>2</sup>NIHR Exeter Clinical Research Facility, University of Exeter Medical School, Exeter, UK

<sup>3</sup>Department of Physical Therapy, East Carolina University, Greenville, NC, USA

<sup>4</sup>Department of Kinesiology, Iowa State University, Ames, IA, USA

<sup>5</sup>Department of Kinesiology, University of Massachusetts, Amherst, MA, USA

## Correspondence

Hannah M. Rice, Sport and Health Science, Richards Building, St Luke's Campus, Heavitree Road, Exeter EX1 2LU, UK.  
Email: H.Rice@exeter.ac.uk

Tibial stress fractures are a problematic injury among runners. Increased loading of the tibia has been observed following prolonged weight-bearing activity and is suggested to be the result of reduced activity of the plantar flexor muscles. The musculature that spans the tibia contributes to bending of the bone and influences the magnitude of stress on the tibia during running. Participant-specific models of the tibia can be used as a non-invasive estimate of tibial stress. This study aimed to quantify tibial stress during running using participant-specific bone geometry and to compare tibial stress before and after a protocol of repeated muscular contractions of the plantar flexor muscle group. Fourteen participants who run recreationally were included in the final analysis of the study. Synchronized force and kinematic data were collected during overground running before and after an exhaustive, weighted calf-raise protocol. Bending moments and stress at the distal third of the tibia were estimated using beam theory combined with inverse dynamics and musculoskeletal modeling. Bone geometry was obtained from magnetic resonance images. There was no difference in stress at the anterior, posterior, medial, or lateral peripheries of the tibia after the calf-raise protocol compared with before. These findings suggest that an exhaustive, repeated calf-raise protocol did not alter tibial stress during running.

## KEYWORDS

biomechanics, forces, musculoskeletal modeling, overuse injury

## 1 | INTRODUCTION

Lower limb stress fractures are a problematic injury that affect runners,<sup>1</sup> with the tibia one of the most common sites of this injury.<sup>2-4</sup> Tibial stress fractures represent the inability of the skeleton to withstand repetitive bouts of mechanical loading. Repetitive loading can lead to microdamage accumulation, and inadequate repair of this is understood to increase the risk of stress fracture.<sup>5</sup> The magnitude of loading

experienced by the bone is important and may be increased throughout an activity as a result of fatigue. In healthy participants, increased tibial strain has been observed following prolonged weight-bearing activity,<sup>6</sup> and increased peak anterior-posterior tibial stress was observed following just 20 minutes of moderate treadmill running.<sup>7</sup> This increased bone loading may increase the risk of stress fracture.<sup>8</sup>

Milgrom et al<sup>6</sup> showed that following both prolonged running and marching, anterior tibial tensional strains increased,

This is an open access article under the terms of the Creative Commons Attribution License, which permits use, distribution and reproduction in any medium, provided the original work is properly cited.

© 2020 The Authors. *Scandinavian Journal of Medicine & Science in Sports* published by John Wiley & Sons Ltd

alongside reduced gastrocnemius isokinetic torque—indicative of plantar flexor muscle fatigue. It has been suggested that regular activity of the gastrocnemius muscles may be important in maintaining “regular bone strains”.<sup>9</sup> Contraction of the triceps surae contributes to posterior bending of the tibia, while their eccentric contraction can act to counter the external dorsiflexor moment during running.<sup>10</sup> Therefore, reduced function of the plantar flexor muscles—the dominant muscle group during the propulsive phase of running stance<sup>11</sup>—has the potential to change the loading environment of the tibia and, therefore, tibial stress. However, the effects of isolated plantar flexor muscle fatigue on bone stress have not been examined.

Due in part to the challenge of quantifying the internal loading environment of the bone, understanding of the factors that increase bone loading is limited. Tibial strain has been measured invasively in humans,<sup>6</sup> but it may be more feasible and appropriate to use biomechanical models to estimate tibial stress.<sup>7,12–14</sup> Beam theory modeling was shown to be a repeatable approach for quantifying within-participant changes in tibial stress.<sup>7</sup> Previous beam theory approaches have modeled a cross-section of the tibia as a hollow ellipse, using literature-based geometric properties or image-based estimates of bone geometry and assuming symmetry in the cross section.<sup>7,12–14</sup> The accuracy of stress calculated using beam theory could be improved by using participant-specific bone geometry and assuming asymmetry of the cross section. Bone geometry has been proposed to be important when understanding risk of stress injury as measures of geometry, including cross-sectional area, section modulus, and area moment of inertia, have been inversely associated with risk of stress fracture in military populations.<sup>15–17</sup>

This study had two separate aims: (a) to estimate tibial stress during running using participant-specific bone geometry; and (b) to compare tibial stress before and after an exhaustive protocol of repeated muscular contractions of the plantar flexor muscle group. It was hypothesized that tibial stress during running would be increased following the calf-raise protocol.

## 2 | MATERIALS AND METHODS

### 2.1 | Participants

Fifteen participants were included in the study (6 female, 9 male; mean (SD) 24.6 (9.7) years; 75.3 (11.6) kg; 1.76 (0.10) m). Sample size was estimated with G\*Power Version 3.1.9.2<sup>18</sup> using previously reported differences in peak anterior stress values in those with and without a history of stress fracture.<sup>12</sup> This was used so that only clinically relevant changes in bone stress would be detected. An alpha level of 0.05 and power of 80% were used to determine sample size.

A sample of 14 was determined to be sufficient for this pre-post study design.

Participants self-reported that they were regularly active (>150 min/wk) and had prior experience of distance running at a recreational level or above. Participants were injury-free at the time of data collection and had no history of stress fracture to the tibia, metatarsals, or femur. All participants provided written informed consent prior to participation in this study that was approved by the University Research Ethics Committee.

### 2.2 | Magnetic resonance (MR) imaging

A stack of transverse MR images covering the whole of the lower leg were acquired using a 1.5 T superconducting whole body scanner (Gyrosan Intera, Philips) with participants lying in a prone position. A T1-weighted (repetition time: 20 ms; echo time: 3.6 ms) 3D gradient echo sequence was utilized with an in-plane resolution of 0.68 x 0.68 mm and a slice thickness of 2 mm.

### 2.3 | MR analysis

Images were processed in ImageJ (1.50i, National Institutes of Health). The proximal and distal ends of the tibia and the slice representing one-third of the length from distal to proximal were identified. This site was used for comparison with previous studies<sup>12,13</sup> as an approximation of the narrowest point of the tibia.<sup>16</sup> A straight line between the most medial and lateral aspects of the medial and lateral malleoli, respectively, was inserted. The angle between this line and the horizontal was used to rotate the image, such that the anterior aspect of the tibia was facing upwards on the screen. This aligned the anterior tibia with the anterior direction of the dynamic tibia coordinate system, determined using motion capture. Cross-sectional area, the second moment of area about the medial-lateral and anterior-posterior axes, and the product second moment of area were obtained using a customized Matlab script.<sup>19</sup> This script utilized an edge detection algorithm to identify the cortical and trabecular bone. A series of triangles were fit to the cortical bone to calculate the bending parameters of the cross section (Figure 1).

### 2.4 | Running protocol

Height and body mass were determined for scaling in the musculoskeletal model. Participants wore their own running footwear, which was self-reported to be the footwear that they run in most regularly at the time of data collection. Eighteen active Codamotion (Charnwood Dynamics Ltd)

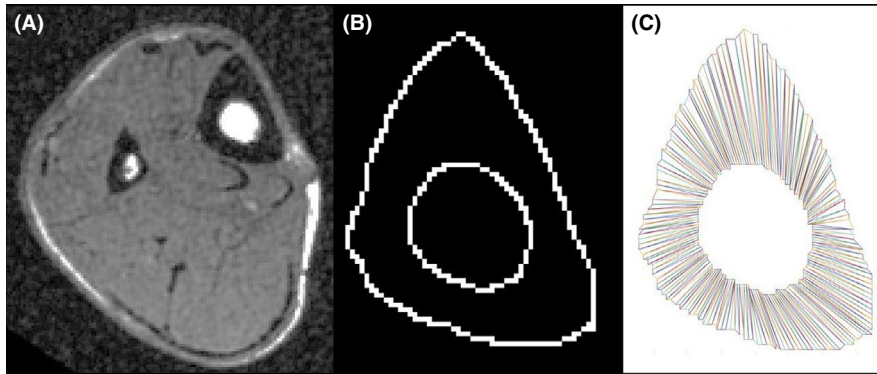


**FIGURE 1** Sample of a digitized tibial cross section utilizing a customized Matlab script.<sup>19</sup> A, MR image of the shank at the distal third of the tibia; B, tibial cross section edges detected; C, triangles fit to the cortical bone. Note: the contrast in (A) has been edited to maximize clarity for presentation purposes only

markers were positioned to identify thigh, lower leg, and foot segments from the right lower limb that were then tracked using four CX1 Codamotion sensor units (12 cameras, 200 Hz). Anatomical markers were placed on the calcaneus, first and fifth metatarsals, medial and lateral malleoli, medial and lateral femoral epicondyles, and the greater trochanter. A static trial was collected with the participant in their comfortable standing position with feet shoulder width apart. Synchronized force data were collected from an AMTI force platform (AMTI) at 1000 Hz. Five overground running trials at  $3.6 \text{ m/s} \pm 5\%$  were collected that included a full right foot contact on the force platform where the stride was judged by the investigator not to have been adjusted in order to contact the platform.

## 2.5 | Calf-raise protocol

Following completion of the initial overground running trials, participants wore a weight vest that contained 10% of their body mass to the nearest 0.5 kg. Participants stood with the balls of their feet on the edge of a step and performed repeated calf raises, plantar flexing maximally and lowering to maximum dorsiflexion. A metronome set at 1.33 Hz was used to guide the participants to rise to maximum plantar flexion in one beat, followed by four beats of controlled lowering to maximum dorsiflexion. Participants were permitted to lightly place their fingertips on a wall less than 0.5 m in front of them for balance. They were asked to pause as briefly as possible to adjust their foot position if they felt they were starting to slip. Participants were given the opportunity to familiarize to this task, both with and without the weight vest, until they felt comfortable. Participants performed repeated calf raises continuously until failure was reached. Failure was defined as three consecutive calf raises during which the full range of motion was not reached, or the correct tempo was not maintained, according to the judgement of investigators. Inability to maintain calf-raise height has been suggested to be indicative of fatigue.<sup>20</sup> Participants were unaware of the criteria for termination of the test.

Encouragement was provided to all participants throughout the calf-raise protocol. The average approximate duration of the calf-raise protocol was  $7 (\pm 3)$  minutes per person.

## 2.6 | Post-calf-raise protocol

An additional five overground running trials were collected immediately following the calf-raise protocol. In between each of these running trials, participants completed ten calf raises without the weight vest, using the same tempo as throughout the calf-raise protocol. This was intended to minimize the effects of recovery. Codamotion markers were worn throughout the entirety of these protocols.

## 2.7 | Data analysis

Kinematic and force data were filtered using a 2nd order low-pass Butterworth filter at 12 Hz.<sup>21</sup> The static trial was used to identify knee and ankle joint centers. Segment mass, center of mass location, and inertial properties were calculated, and joint moments were determined using inverse dynamics within Codamotion Odin software. Foot strike was determined from the vertical force time histories and used to categorize runners as rearfoot strikers (displaying a distinct impact peak) and non-rearfoot strikers (displaying no distinct impact peak).<sup>22</sup>

## 2.8 | Stress model

A customized Matlab (R2017a, MathWorks) program was written to estimate tibial stress and has been detailed by Rice et al.<sup>7</sup> In brief, segment center of mass accelerations and joint reaction forces were calculated. Bending due to muscular forces was calculated from nine muscles that span the cross section at the distal third of the tibia: Tibialis Anterior; Soleus; Tibialis Posterior; Extensor Digitorum Longus; Flexor Digitorum Longus; Flexor Hallucis

Longus; Peroneus Brevis; Peroneus Longus; and Extensor Hallucis Longus. Dynamic muscle forces were estimated using static optimization with a cost function minimizing the sum of cubed muscle stresses.<sup>23</sup> The two gastrocnemii muscles span the tibial cross section but originate on the femur. Therefore, they were assumed to contribute to axial compression but not to bending of the tibia. The axial and bending contributions from each muscle were calculated in both the anterior-posterior and medial-lateral directions. The bending due to the muscles crossing the centroid was the product of the muscular forces and their respective moment arms. The bending at the centroid due to the external reaction forces included the contributions from both the knee joint reaction force and the knee joint moment (termed contact forces).

As in Rice et al.,<sup>7</sup> stance phase axial and bending forces due to the external reaction forces and internal muscular forces were vector summed to represent the resultant axial force and resultant bending moments acting at or about the centroid at the distal third of the tibia. Normal stresses at the posterior, anterior, lateral, and medial peripheries were calculated as axial stress  $\pm$  bending stress. The Matlab program was adapted to account for the geometric properties of the tibia cross section in order to estimate the axial and bending stress. Axial stress was the resultant axial force divided by the participant-specific cross-sectional area of the distal third of the tibia.

Anterior-posterior and medial-lateral bending stresses ( $\sigma_{BE\_Anterior}$ ,  $\sigma_{BE\_Posterior}$ ,  $\sigma_{BE\_Lateral}$ ,  $\sigma_{BE\_Medial}$ ) were estimated using the following Equation<sup>24</sup>:

$$\sigma_{BE\_Anterior} = \frac{M_{ML} I_{AP} - M_{AP} I_{xy}}{I_{ML} I_{AP} - I_{xy}^2} y_A$$

$$\sigma_{BE\_Posterior} = \frac{M_{ML} I_{AP} - M_{AP} I_{xy}}{I_{ML} I_{AP} - I_{xy}^2} y_P$$

$$\sigma_{BE\_Lateral} = \frac{M_{AP} I_{ML} - M_{ML} I_{xy}}{I_{ML} I_{AP} - I_{xy}^2} x_L$$

$$\sigma_{BE\_Medial} = \frac{M_{AP} I_{ML} - M_{ML} I_{xy}}{I_{ML} I_{AP} - I_{xy}^2} x_M$$

where  $M_{ML}$  and  $M_{AP}$  refer to the bending moments about the medial-lateral and anterior-posterior axes, respectively;  $I_{ML}$ ,  $I_{AP}$ , and  $I_{xy}$  refer to the second moment of area about the medial-lateral and anterior-posterior axes and product second moment of area, respectively; and  $x_L$ ,  $x_M$ ,  $y_A$ ,  $y_P$  refer to the distances from the centroid to the lateral, medial, anterior, and posterior peripheries, respectively.

## 2.9 | Statistical analysis

For each participant, the most representative trial from each condition (pre- and post-) was obtained using a functional measure of depth,<sup>25</sup> and the bending moments and stress time histories from this trial were utilized in statistical analyses. This avoided the shape distortion of the curve that occurs when taking the mean of multiple trials. SPM analyses allowed comparison of time histories, normalized to 101 data points, for bending moments and stress at the four peripheral sites pre- and post-calf-raise protocol. SPM analyses were carried out using open-source SPM1d Matlab code (<http://www.spm1d.org>).<sup>26</sup> One-tailed paired *t* tests were conducted to compare group mean time histories pre- and post-calf-raise protocol using an alpha level of 0.05.

Comparison of discrete peak values between pre- and post-calf-raise protocol was conducted in IBM SPSS Statistics for Windows (IBM Corp., Version 24.0.). Wilcoxon signed-rank tests identified any differences post- compared with pre-calf-raise protocol. These non-parametric tests were selected due to the non-normality of the discrete data. An alpha level of 0.05 was used.

## 3 | RESULTS

Ten participants ran with a rearfoot strike and four ran with a non-rearfoot strike, maintaining a consistent foot strike in both the pre- and post-calf-raise protocol conditions. One participant changed their foot strike following the protocol and was excluded from the analyses. The analyzed participants ( $n = 14$ ) included 6 females and 8 males with a mean (SD) age of 25.0 (10.0) years, mass of 74.0 (11.3) kg, and height of 1.74 (0.09) m.

### 3.1 | Bending moments

Resultant bending moments about the medial-lateral axis (contributing to anterior-posterior stress) were predominantly in the positive anticlockwise direction throughout stance (Figure 2A). There were no differences in bending moments about the medial-lateral axis pre- compared with post-fatiguing protocol throughout stance and no difference in peak bending moments (Mean (SD) pre-: 105.6 (35.6) N•m; post-: 112.3 (45.0) N•m;  $P = .149$ ). Peak bending moments about the medial-lateral axis provided a relative contribution of 76% ( $\pm 7\%$ ) to peak posterior compressive stress.

There was considerable variability in the bending moments about the anterior-posterior axis (contributing to medial-lateral stress; Figure 3). The resultant was predominantly in the positive anticlockwise direction throughout stance (Mean (SD) peak resultant bending moments pre-:



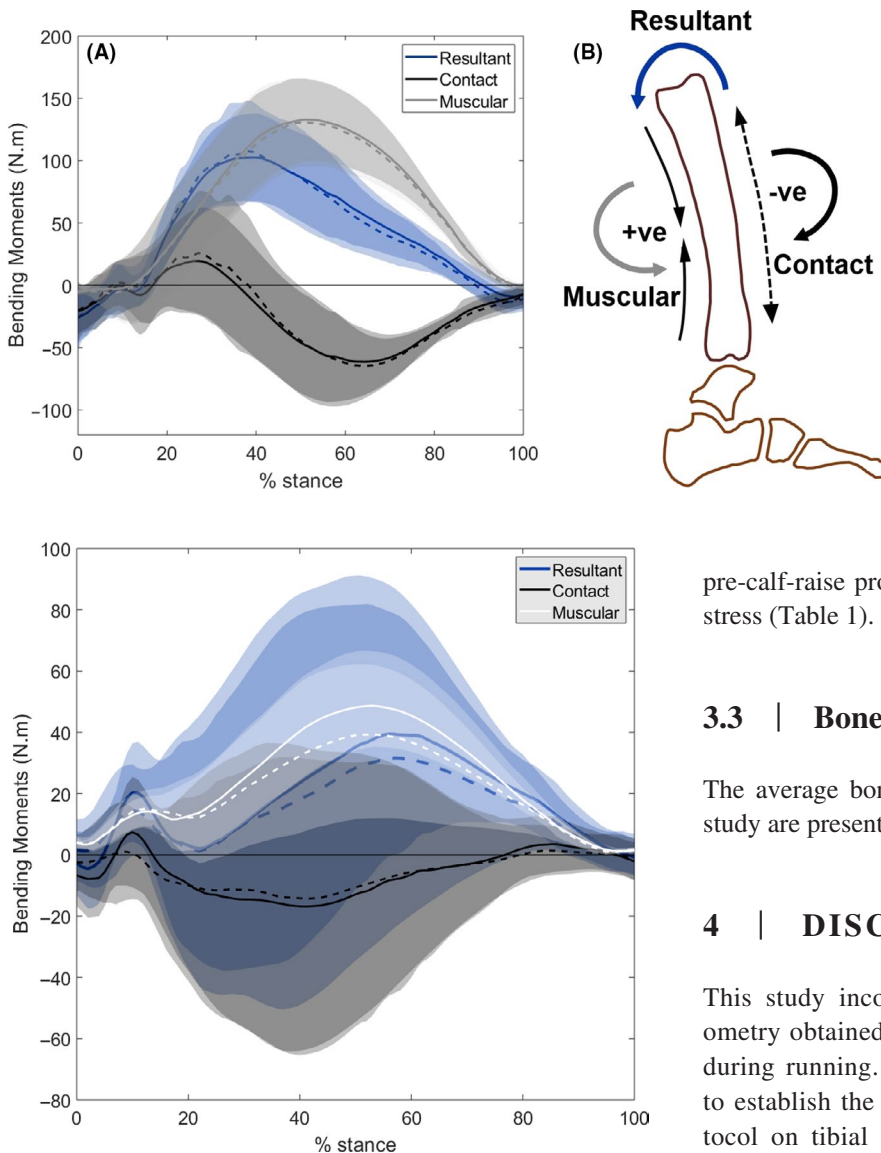


**FIGURE 2** A, Mean and standard deviation time histories of bending moments about the medial-lateral axis during stance; B, the positive resultant bending moment indicates posterior compression and anterior tension. Shading around the mean curve represents the standard deviation. Solid and dashed lines represent pre- and post-fatiguing protocol, respectively

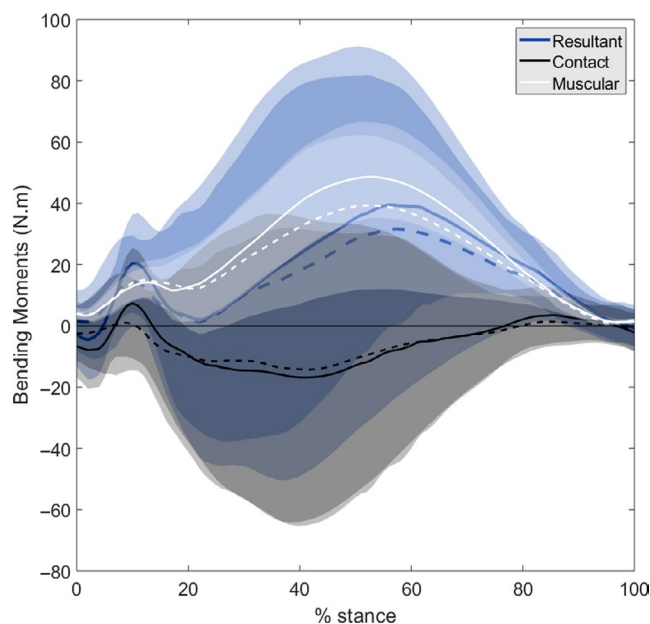


**FIGURE 3** Mean time histories of bending moments about the anterior-posterior axis during stance. The positive resultant bending moment indicates medial compression and lateral tension. Shading around the mean resultant bending moment curve represents the standard deviation. Solid and dashed lines represent pre- and post-fatiguing protocol, respectively

52.0 (33.6) N•m; post-: 54.0 (38.4) N•m). However, a predominantly positive resultant was observed in eight of the fourteen participants, with the remaining six participants showing predominantly negative resultant bending moments.

### 3.2 | Peripheral stress

There was no difference in stress at the anterior, posterior, lateral, or medial peripheries of the tibia post- compared with

pre-calf-raise protocol (Figure 4) and no difference in peak stress (Table 1).

### 3.3 | Bone size

The average bone geometry values for participants in this study are presented for descriptive purposes (Table 2).

## 4 | DISCUSSION

This study incorporated individual participant bone geometry obtained from MR images to quantify tibial stress during running. These stress values were then compared to establish the influence of an exhaustive calf-raise protocol on tibial stress. As in previous studies,<sup>7,9,12-14</sup> the resultant bending moments about the medial-lateral axis were positive, interpreted as tending to bend the tibia in a concave posterior manner (Figure 2B). This is indicative of predominantly tensile stresses on the anterior tibia and predominantly compressive stresses on the posterior tibia during stance. The bending about the anterior-posterior axis revealed individual differences regarding whether the medial or lateral tibia was predominantly under tension, where a positive resultant bending moment would be indicative of tensile stresses on the lateral tibia and compressive stresses on the medial tibia. Our observations agree with Meardon and Derrick<sup>13</sup> that there is considerable between-participant variability in stress magnitudes, particularly at the medial and lateral peripheries. However, peak stresses at the anterior and posterior tibia were lower than previously reported values obtained using a similar modeling approach.<sup>7,12,13</sup> This is influenced by the greater cross-sectional geometry values in the present study than in previous studies. Franklyn et al<sup>27</sup> reported cross-sectional areas of 340 mm<sup>2</sup> (averaged across active males and females)

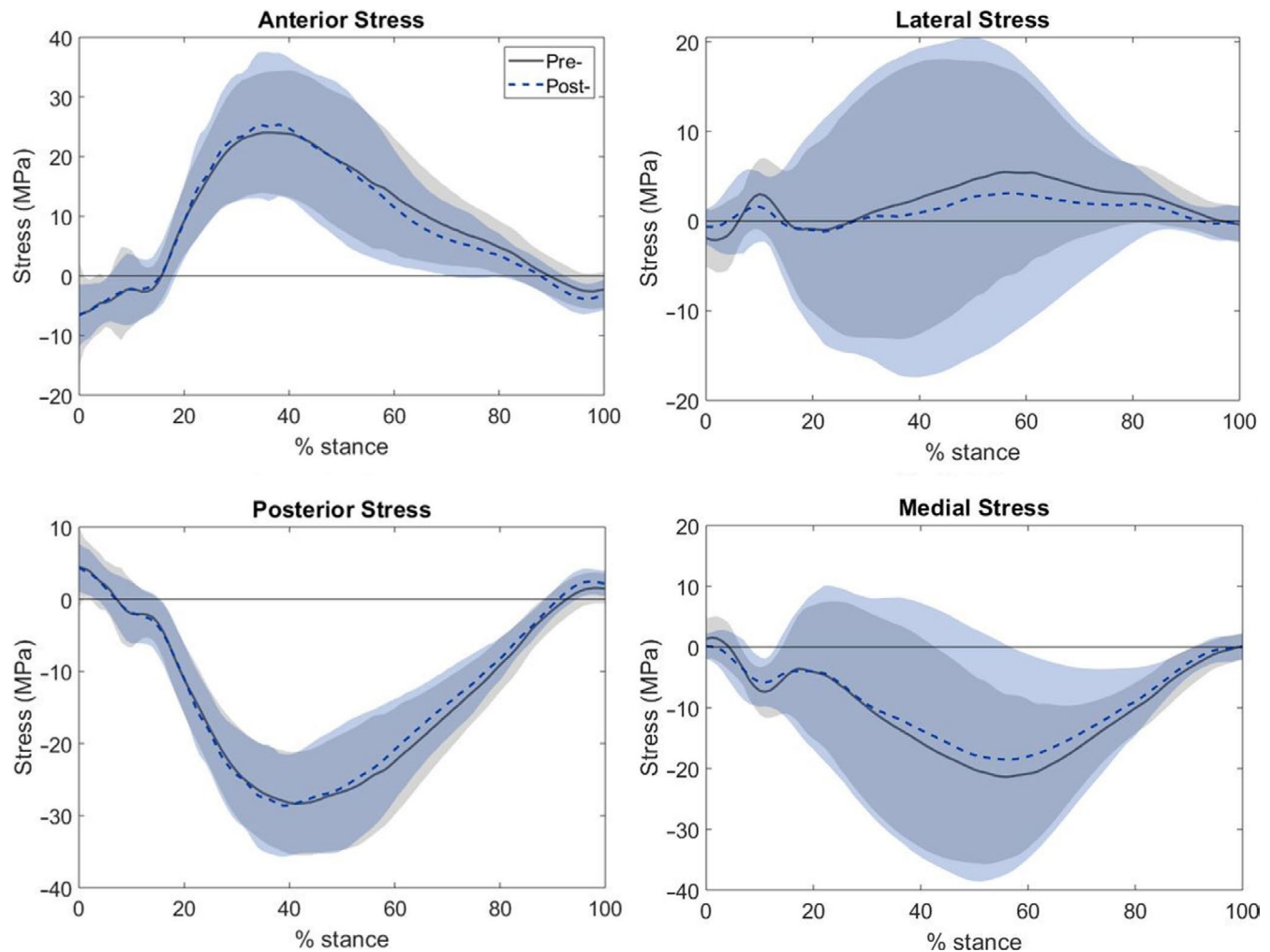


**FIGURE 4** Mean and standard deviation stress time histories at the anterior, posterior, lateral, and medial peripheries of the distal one-third tibial cross section

**TABLE 1** Mean (SD) peak stress at the anterior, posterior, medial, and lateral peripheries of the distal third of the tibia, pre- and post-calf-raise protocol

	Pre-	Post-	<i>P</i>
Peak anterior stress (MPa)	25.1 (10.6)	26.6 (13.3)	.551
Peak posterior stress (MPa)	-29.3 (7.7)	-30.1 (8.6)	.594
Peak lateral stress (MPa)	10.5 (9.2)	10.9 (11.0)	.875
Peak medial stress (MPa)	-23.9 (12.8)	-23.8 (15.3)	.510

compared with 740 mm<sup>2</sup> in the present study. They also reported an outer anterior-posterior width of 30.2 mm compared with 38.3 mm in the present study. These discrepancies may be due to the different scanning techniques or the fact that more points were used to digitize the bone in the present study.

**TABLE 2** Mean (SD) cross-sectional area, second moment of area about the medial-lateral ( $I_{ML}$ ) and anterior-posterior ( $I_{AP}$ ) axes, and product second moment of area ( $I_{xy}$ ) of the cross section at the distal third of the tibia

Variable	Mean (SD)
Cross-sectional area (m <sup>2</sup> )	7.4 (1.0) e <sup>-4</sup>
$I_{ML}$ (m <sup>4</sup> )	8.9 (2.9) e <sup>-8</sup>
$I_{AP}$ (m <sup>4</sup> )	6.2 (2.3) e <sup>-8</sup>
$I_{xy}$ (m <sup>4</sup> )	-1.4 (1.5) e <sup>-8</sup>

In order to further investigate this, bending moment and axial force values from the present study were input into a hollow elliptical stress calculation using previously reported literature values.<sup>27</sup> This revealed peak anterior and posterior stress magnitudes that were double those of the present study and therefore more similar to previously reported stress values. Peak bending moments about both axes were similar in magnitude to previously reported values.<sup>7</sup> It is not possible

to directly validate these stress magnitudes, and therefore, beam theory modeling approaches remain best suited for the assessment of within-participant changes in bone loading. Nonetheless, previous estimates of bone stress using elliptical models may have been overestimated.

It has been suggested that the increased anterior tibial strain previously observed following prolonged activity was the result of plantar flexor muscle fatigue.<sup>6</sup> While fatigue was not defined in the present study, the results suggest that repeated and demanding plantar flexor muscle activity did not increase loading of the tibia, in contrast to the hypothesis. The sensitivity of the tibial stress model to detect changes in tibial stress must be considered in this context. A similar modeling approach showed that in repeated tibial stress measures a difference of 4% and 2% in peak anterior and posterior stress was observed, respectively, between sessions.<sup>7</sup> Furthermore, this approach was able to detect significant increases of 15% and 12% in peak anterior and posterior stress, respectively, throughout a moderate treadmill run. Additionally, this difference was observed in more than 86% of the participants. In contrast, in the present study, the average (non-significant) change in peak anterior and posterior stress was +3% with 43% of participants demonstrating decreased stress. This suggests that the robustness of the model to detecting changes in stress was unlikely to explain why no differences were observed post- compared with pre-calf-raise protocol.

The calf-raise protocol may have been insufficiently demanding to elicit changes in tibial loading. To assess this suggestion, individual responses were considered. Ten out of 14 participants (71%) ran with reduced bending due to muscular forces following the fatiguing protocol, and this was unrelated to foot strike. When comparing stress pre- and post-calf-raise protocol in only these 10 participants, there was a 4% reduction in peak bending due to muscular forces post-compared with pre-protocol ( $P = .005$ ), but no differences in peak tibial stress at any of the four peripheries. Furthermore, participants anecdotally reported that they experienced delayed onset muscle soreness in the days following the protocol. A more robust indicator of the perceived severity of the protocol would have been beneficial.

The changes in tibial loading previously reported following a prolonged activity<sup>6,7</sup> may have been induced via a different mechanism and not the result of plantar flexor fatigue per se. Theoretically, it is to some extent counterintuitive that reduced activity of the plantar flexor muscles would result in increased tibial loading. Experimental data using bone screws to quantify tibia segment deformation,<sup>9</sup> as well as beam bending models,<sup>7,12-14</sup> have suggested that the proximal tibia bends posteriorly during running. This implies that reduced activity of the plantar flexor muscles would contribute to a reduction in the bending observed, thereby reducing strain in the tibia. In reality, there are many factors that may

influence the loading environment, including the fact that the gastrocnemius muscles are biarticular and also contribute to knee flexion-extension. It should be noted that the plantar flexor muscles additionally act eccentrically during stance to counter the external dorsiflexor moment. This complex loading environment in conjunction with the findings from the present study indicates that the increased bone loading previously observed following prolonged weight-bearing activity may not simply be the result of plantar flexor muscle fatigue.

## 4.1 | Limitations

Modeling the tibia using beam theory provides a non-invasive approach that may be important for improving understanding of the mechanisms of tibial stress fracture development. Utilizing such an approach to quantify within- rather than between-participant differences in stress is most appropriate. There are a number of limitations that must be considered. In order to quantify the contributions from muscular forces, simplifications have been introduced. In particular, using static optimization to estimate muscular forces assumes standardized force capabilities and neural strategies. Participant-specific estimates of model parameters, such as muscle moment arms, would improve the accuracy of the model. Additionally, modeling the foot with multiple segments rather than a single, rigid segment would better represent the kinematics.

In terms of the study design, the protocol was a simplified means of reducing the function of the plantar flexor muscles, and while “failure” was reached according to the assessment of the investigators, fatigue was neither defined nor quantified. It was possible to assess plantar flexor torque using a dynamometer but this would have introduced considerable recovery time that may have interfered with the intended effects of the calf-raise protocol, to the detriment of the study overall. The protocol focused on eliciting a change in the mechanical environment, without consideration of the physiology. The relative contributions of the gastrocnemii and soleus muscles during running and during the protocol were not considered, nor were their different fiber type composition. A more in-depth physiological assessment may provide further insight into the findings of the present study.

This study included both rearfoot and non-rearfoot strike runners which provides a useful representation of the running population but meant that differences between these different categories of runner were not accounted for. However, strike index was retrospectively determined from foot strike angle and bivariate correlation analyses showed there was no association between strike index and peak stress at any of the peripheries, nor between strike index and the peak resultant bending moments. Data were collected at a pre-determined speed that may not represent the speed participants were most

accustomed to. Whether the results may have been different at self-selected running speeds remains unclear.

## 5 | PERSPECTIVE

An exhaustive protocol of repeated, weighted calf raises did not induce changes in tibial stress during running, suggesting that baseline tibial loading magnitudes can be maintained during running even when the plantar flexor muscle group functionality has been altered. The role of the plantar flexor muscles in maintaining a normal tibial loading environment remains poorly understood.

## ACKNOWLEDGEMENTS

The authors would like to acknowledge the contributions of Dr Garry Massey and Sam Wisdich to this work.

## ORCID

Hannah M. Rice  <https://orcid.org/0000-0002-7479-6924>

Matthew A. Ellison  <https://orcid.org/0000-0003-1804-328X>

Stacey A. Meardon  <https://orcid.org/0000-0002-9963-2985>

Timothy R. Derrick  <https://orcid.org/0000-0002-3234-7936>

## REFERENCES

- Robertson GAJ, Wood AM. Lower limb stress fractures in sport: Optimising their management and outcome. *World J Orthop.* 2017;8(3):242-255.
- Iwamoto J, Takeda T. Stress fractures in athletes: review of 196 cases. *J Orthop Sci.* 2003;8(3):273-278.
- Bruckner P, Bradshaw C, Khan KM, White S, Crossley K. Stress fractures: a review of 180 cases. *Clin J Sport Med.* 1996;6(2):85-89.
- Kiel J, Kaiser K. *Stress Reaction and Fractures*. Treasure Island, FL: StatPearls. StatPearls Publishing; 2018. Accessed July 25, 2018.
- Burr DB. Why bones bend but don't break. *J Musculoskelet Neuronal Interact.* 2011;11(4):270-285.
- Milgrom C, Radeva-Petrova D, Finestone A, et al. The effect of muscle fatigue on in vivo tibial strains. *J Biomech.* 2007;40(4):845-850.
- Rice H, Weir G, Trudeau MB, Meardon S, Derrick T, Hamill J. Estimating tibial stress throughout the duration of a treadmill run. *Med Sci Sports Exerc.* 2019;51(11):2257-2264.
- Edwards WB, Taylor D, Rudolph TJ, Gillette JC, Derrick TR. Effects of running speed on a probabilistic stress fracture model. *Clin Biomech Bristol Avon.* 2010;25(4):372-377.
- Yang P-F, Sanno M, Ganse B, et al. Torsion and antero-posterior bending in the in vivo human tibia loading regimes during walking and running. *PLoS One.* 2014;9(4):e94525.
- Mann RA, Hagy J. Biomechanics of walking, running and sprinting. *Am J Sports Med.* 1980;8(5):787-797.
- Hamner SR, Seth A, Delp SL. Muscle contributions to propulsion and support during running. *J Biomech.* 2010;43(14):2709-2716.
- Meardon SA, Willson JD, Gries SR, Kernozek TW, Derrick TR. Bone stress in runners with tibial stress fracture. *Clin Biomech.* 2015;30(9):895-902.
- Meardon SA, Derrick TR. Effect of step width manipulation on tibial stress during running. *J Biomech.* 2014;47(11):2738-2744.
- Derrick TR, Edwards WB, Fellin RE, Seay JF. An integrative modeling approach for the efficient estimation of cross sectional tibial stresses during locomotion. *J Biomech.* 2016;49(3):429-435.
- Beck TJ, Ruff CB, Mourtada FA, et al. Dual-energy X-ray absorptiometry derived structural geometry for stress fracture prediction in male U.S. Marine Corps recruits. *J Bone Miner Res.* 1996;11(5):645-653.
- Milgrom C, Giladi M, Simkin A, et al. The area moment of inertia of the tibia: a risk factor for stress fractures. *J Biomech.* 1989;22(11-12):1243-1248.
- Beck TJ, Ruff CB, Shaffer RA, Betsinger K, Trone DW, Brodine SK. Stress fracture in military recruits: gender differences in muscle and bone susceptibility factors. *Bone.* 2000;27(3):437-444.
- Faul F, Erdfelder E, Lang A-G, Buchner A. G\*Power 3: a flexible statistical power analysis program for the social, behavioral, and biomedical sciences. *Behav Res Methods.* 2007;39(2):175-191.
- Kenny M, Ellison M, Rice HM. Matlab code to digitise MR bone images and calculate properties of shape: cross-sectional area, area moment of inertia, product moment of area. Published online September 2, 2019. <https://doi.org/10.24378/exe.1763>
- Hébert-Losier K, Newsham-West RJ, Schneiders AG, Sullivan SJ. Raising the standards of the calf-raise test: a systematic review. *J Sci Med Sport.* 2009;12(6):594-602.
- Bisseling RW, Hof AL. Handling of impact forces in inverse dynamics. *J Biomech.* 2006;39(13):2438-2444.
- Cavanagh PR, LaFortune MA. Ground reaction forces in distance running. *J Biomech.* 1980;13(5):397-406.
- Erdemir A, McLean S, Herzog W, van den Bogert AJ. Model-based estimation of muscle forces exerted during movements. *Clin Biomech.* 2007;22(2):131-154.
- Cook RD, Young WC. *Advanced Mechanics of Materials*. Upper Saddle River, NJ: Prentice Hall; 1999.
- Sangeux M, Polak J. A simple method to choose the most representative stride and detect outliers. *Gait Posture.* 2015;41(2):726-730.
- Pataky TC, Robinson MA, Vanrenterghem J. Region-of-interest analyses of one-dimensional biomechanical trajectories: bridging 0D and 1D theory, augmenting statistical power. *PeerJ.* 2016;4:e2652.
- Franklyn M, Oakes B, Field B, Wells P, Morgan D. Section modulus is the optimum geometric predictor for stress fractures and medial tibial stress syndrome in both male and female athletes. *Am J Sports Med.* 2008;36(6):1179-1189.

**How to cite this article:** Rice HM, Kenny M, Ellison MA, et al. Tibial stress during running following a repeated calf-raise protocol. *Scand J Med Sci Sports.* 2020;30:2382-2389. <https://doi.org/10.1111/sms.13794>